Available online at www.sciencedirect.com
ScienceDirect
Ceramics International 34 (2008) 1247–1252
CERAMICS INTERNATIONAL
www.elsevier.com/locate/ceramint

# Effects of zirconium silicate and chromite addition on the microstructure and bulk density of magnesia–magnesium aluminate spinel-based refractory materials

P.G. Lampropoulou, C.G. Katagas *

*Department of Geology, University of Patras, 26500 Patras, Greece*

Received 22 August 2006; received in revised form 24 February 2007; accepted 4 March 2007
Available online 18 April 2007

**Abstract**

Six synthesized magnesium aluminate spinel-based refractory compositions used in steel and cement applications, were prepared using a two stage sintering process at 1760 °C, starting with approximately 1:1 wt% ratio of pure magnesia and alumina with additions of zirconium silicate (0.5, 1.0 and 2.0 wt%) and chromite (2.0, 3.0 and 5.0 wt%). These compositions were investigated for effects on densification, chemical and mineralogical phases formed.

The results show that free periclase, along with the magnesium aluminate spinel, is present in all samples. In samples with zirconium silicate additives, the high melting phase $CaZrO_3$ was formed, promoting densification and refractoriness; but also controlling the occurrence of calcium aluminate and calcium silicate phases. Zirconium silicate also caused the bulk density to increase in all samples. In samples with chromite additive, $Cr^{3+}$ (and $Fe^{3+}$) enters the spinel lattice, substituting for $Al^{3+}$ ions, and accelerated the spinel formation as well as increased the density of the crystals and their direct bonding. The bulk density of samples with chromite additives increased with the amount of additive.

*Keywords:* Magnesium aluminate spinel; Additives; Mineralogical compositions; Microstructures

## 1. Introduction

Magnesium aluminate (MA) spinel is a refractory material with excellent high-temperature properties that is successfully used as a raw material for the production of linings for ladles of steel furnaces and in the hot-zone of cement rotary kilns and roofs. Moreover, contrary to magnesium chromite refractories, MA spinel refractories are very attractive due to their environmental friendliness.

The effects of different additives on the development of MA refractories has been studied by a number of researchers. Oxides additives such as $Y_2O_3$ [1] and $Yb_2O_3$ [2] were reported to improve the sintered properties of magnesium aluminate spinel; and according to Baik [3], $TiO_2$ improved the densification of the spinel microstructure more than $MnO_2$. In addition, Sarkar and Bannerjee [4] observed a gradual improvement of densification of MA spinel with additions of $TiO_2$ up to 1.5 mass% at 1500 °C, whereas higher amounts of $TiO_2$ reduced the density. According to Sarkar et al. [5], the addition of $TiO_2$ showed greater refractoriness than $Cr_2O_3$, $V_2O_5$, or $B_2O_3$ additives. Ghosh et al. [6] found that an addition of 1 wt% ZnO is optimal for the best densification, hot strength and thermal shock resistance. $Cr_2O_3$ has been also reported to improve the thermal shock and corrosion resistance [7–9], as well as the densification of MA spinels [10]. $ZrO_2$ additions greater than 1.4% have been observed to improve the densification of spinels [11], whilst according to Yang et al. [12], additives of $ZrO_2$ increase the resistance to cold crushing strength as well as to thermal shock.

The relevant literature lacks detailed systematic research on the effects of different amounts of chromite or zirconium silicate additions on the mineralogical and physical properties of spinel-based compositions. This study was undertaken to determine how these additives affect the mineralogical composition, the chemistry of the coexisting phases, and the refractory behavior of MA spinel-based refractory materials.

---

* Corresponding author. Tel.: +30 2610997596; fax: +30 2610997596.
*E-mail address:* c.katagas@upatras.gr (C.G. Katagas).

0272-8842/$34.00 © 2007 Elsevier Ltd and Techna Group S.r.l. All rights reserved.
doi:10.1016/j.ceramint.2007.03.015

## 2. Experimental procedure

Sintered magnesite (pure magnesia, $MgO > 96\%$) and alumina ($Al_2O_3 > 99.5\%$) obtained from Viomagn, Evia Greece and Aluminum of Greece (Pechiney), Viotia Greece, respectively, were used as raw materials for this study. Low amounts of $SiO_2$ (0.79 wt%), $Al_2O_3$ (0.03 wt%), CaO (2.56 wt%) and MnO (0.04 wt%) were present as impurities in the magnesia.

Commercial quality of zirconium silicate ($ZrSiO_4$) with 32 wt% $SiO_2$ and chromite from Africa, with a composition $(Mg_{0.48}Fe_{0.54})(Cr_{1.18}Al_{0.57}Fe_{0.22})O_4$, were used as additives. The chemical analyses of the chromite ore indicated the presence of a solid solution between chromite, iron spinel and magnesium aluminate spinel.

Six batch compositions were prepared containing pure magnesia and alumina in about 1:1 wt% ratio. In three of them, zirconium silicate was used as additive in proportions of 0.5, 1.0 and 2.0 wt%; and were labelled as 0.5ZrS, 1ZrS and 2ZrS, respectively. The three samples with chromite additions of 2.0, 3.0 and 5.0 wt% were labelled as 1Chr, 2Chr and 3Chr, respectively.

The raw materials were attrition-milled to obtain grain fractions finer than 0.1 mm for magnesia, 0.25 mm for alumina and 0.2 mm for zirconium silicate and chromite. This was followed by mixing the different compositions for 10 min in a laboratory mixer with a binding agent. After mixing, the compositions were pressed in a hydraulic press at 640 kp/cm$^2$, forming cylindrical samples 5 cm in diameter and 10 cm in length. The samples were then dried at 110 °C and sintered up to 1760 °C in a rotary kiln, then furnace cooled. The complete cycle of firing and cooling to room temperature lasted 72 h and formed a dense grain.

As a second stage, the sintered samples were milled again to a grain size finer than 200 mesh. Calcined powders of each mix were shaped in a hydraulic press at 1200 kp/cm$^2$ to cylindrical samples of the same dimensions and sintered in a rotary kiln under the same conditions used in the first sintering.

The raw materials and the synthesized samples were characterized in terms of their bulk composition, chemical composition of coexisting phases, microstructure, and bulk density.

XRF and ICP were used for the chemical analyses of the raw materials and synthesized samples, respectively, while the bulk density was evaluated by the standard liquid method according to ASTM, designation C 373-88 (Reapproved 1994).

All samples were thin sectioned, polished, carbon coated, and examined in backscattered and secondary imaging modes with a JEOL 6300 SEM fitted with ED and WD spectrometers. Powder XRD, EDS or combined EDS and WDS analyses were carried out in order to identify and determine the composition of coexisting phases.

## 3. Results and discussion

### 3.1. Chemical analyses

Chemical analyses of the synthesized spinel-based compositions used in this investigation are given in Table 1. The samples contain low amounts of impurities, decreasing the probability of forming low melting phases.

Table 1
Chemical analyses of synthesised spinel-based materials after firing at 1760 °C with zirconium silicate and chromite additives

| Oxides (wt%) | 0.5ZrS | 1ZrS | 2ZrS | 2Chr | 3Chr | 5Chr |
|---|---|---|---|---|---|---|
| $SiO_2$ | 0.55 | 0.65 | 0.84 | 0.34 | 0.32 | 0.34 |
| $Al_2O_3$ | 46.28 | 47.91 | 47.63 | 47.62 | 45.49 | 45.48 |
| $Fe_2O_3$ | 2.51 | 1.76 | 1.15 | 1.44 | 2.17 | 2.00 |
| MnO | 0.03 | 0.02 | 0.02 | 0.02 | 0.03 | 0.03 |
| MgO | 48.34 | 47.4 | 47.58 | 48.00 | 48.81 | 48.60 |
| CaO | 1.76 | 1.83 | 1.78 | 1.64 | 1.79 | 1.64 |
| $Na_2O$ | 0.02 | 0.00 | 0.00 | 0.01 | 0.01 | 0.02 |
| $K_2O$ | 0.06 | 0.00 | 0.07 | 0.02 | 0.03 | 0.10 |
| $TiO_2$ | 0.00 | 0.002 | 0.004 | 0.01 | 0.01 | 0.02 |
| $P_2O_5$ | 0.00 | 0.00 | 0.00 | 0.00 | 0.00 | 0.00 |
| $Cr_2O_3$ | 0.25 | 0.18 | 0.09 | 0.88 | 1.33 | 2.00 |
| $ZrO_2$ | 0.19 | 0.41 | 0.81 | n.a. | n.a. | n.a. |

n.a.: not analysed; ZrS: zirconium silicate; Chr: chromite.

### 3.2. Bulk density

Fig. 1 shows the variation of their bulk density in terms of different kinds and amounts of additive. Additions of zirconium silicate had a large impact on bulk density, increasing from 3.32 to 3.35 g/cm$^3$ when the quantity increased from 0.5 to 1.0 wt%. Additional increases (2.0 wt%) did not improve the density. Increasing additions of chromite (from 2 to 5 wt%) to the spinel composition were found to increase the bulk density (from 3.32 to 3.34 g/cm$^3$).

### 3.3. XRD and SEM analysis

The mineralogical composition of all samples, determined by XRD and/or SEM analyses are given in Table 2. In all samples, periclase has been detected to coexist with magnesium aluminate spinel crystals. SEM was used to confirm the occurrence of less abundant Ca, Al and Mg-silicate phases not readily detected by powder XRD methods. The minor constituent phases are confined to small regions of the microstructures, posing serious

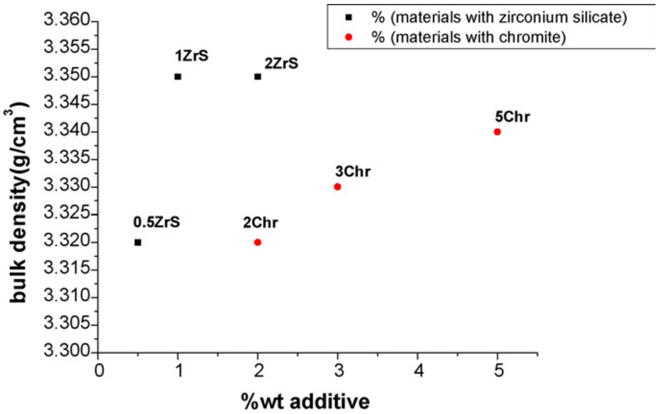

Fig. 1. The variation of bulk density in M-MA spinel-based materials with different proportions (wt%) of zirconium silicate and chromite additives.

Table 2
Coexisting phases in the synthesised spinel-based materials after firing at 1760 °C with zirconium silicate and chromite additives

| Sample | Phases[a] | | | | | | | | | | | | |
|---|---|---|---|---|---|---|---|---|---|---|---|---|---|
| | MA | M | $C_3MS_2$ | $C_3S_2$ | $C_2S$ | $C_3S$ | C | CA | $C_3A$ | $C_{12}A_7$ | $CF_2$ | $C_2AS$ | CZr |
| 0.5ZrS | ma[b] | ma | | ++[c] | ++ | ++e | ++e | | +++e | + | cp[d] | | ++e |
| 1ZrS | ma | ma | | +++ | +++e | +e | ++ | | +e | + | cp | + | ++e |
| 2ZrS | ma | ma | +++ | +++ | +e | | | +e | | +e | cp | + | ++e |
| 2Chr | ma | ma | | +++ | +++e | +e | ++e | | ++e | + | cp | + | |
| 3Chr | ma | ma | | +++ | +++e | ++e | ++e | | ++e | + | cp | + | |
| 5Chr | ma | ma | | +++ | +++e | ++e | +e | | ++e | + | cp | + | |

[a] M: MgO; A: $Al_2O_3$; C: CaO; F: $Fe_2O_3$; Zr: $ZrO_2$; S: $SiO_2$.

[b] ma: major phases.

[c] Minor constituent phases—+++: abundant; ++: frequent; +: sparse; e: stable phase expected to be present.

[d] cp: contingent phase.

problems in obtaining fully quantitative chemical analyses of them. However, special care has been taken to obtain analyses which are either stoichiometric or approximate closely the stoichiometry.

The stabilizing additive of zirconium silicate favored the formation of the high melting point phase $CaZrO_3$, which should improve the overall refractoriness of the materials. Moreover, the zirconium silicate additive seems to control the formation, the amount and the type of other minor phases. It is evident from the data presented in Table 2, that in samples with progressively higher amounts of zirconium silicate additives, the calcium–silicate phases are more abundant than the calcium–aluminate ones. In samples with 1.0 wt% zirconium silicate additions, the $C_2S$ and $C_3S_2$ phases (with melting points 2130 and 1475 °C, respectively) are more frequent, whereas, with 2.0 wt% additions, the most abundant phases are the low melting phases $C_3S_2$ and $C_3MS_2$ (melting point: 1550 °C). It is worth noting that very low amounts of the phases $C_3S_2$, $C_2S$, $C_3S$ and $C_3A$ were formed in samples with chromite additive.

More than 30 spot SEM microanalyses (spot size <5 μm) of spinel crystals were performed in every sample and representative analyses from each sample, recalculated on the basis of 32(O) per formula unit, are presented in Table 3. The analytical data presented in this table suggest that the spinel crystals from the chromite added samples have lower mean $Al_2O_3$ wt% values than those from samples with zirconium silicate. It is also evident that additions of various amount of chromite have a remarkable impact on the chemical composition of the spinel crystals formed in each sample. This is thought to be a result of Cr and Fe ions substituting for Al in the spinel lattice. $Cr_2O_3$, enters the lattice of spinel by solid solution, increasing the crystal density, compared to spinels

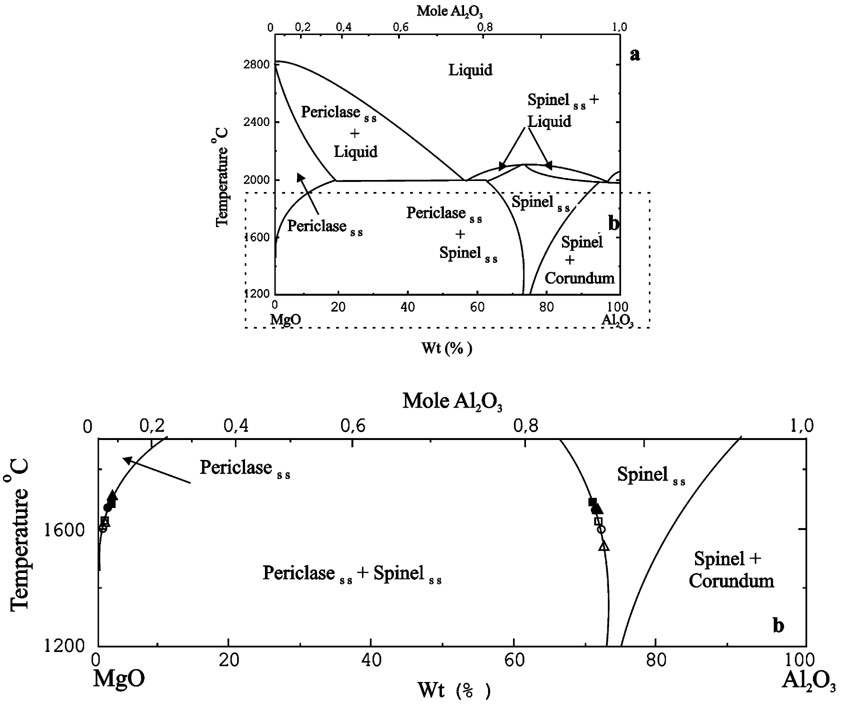

Fig. 2. Plots of coexisting spinel and periclase chemical compositions on the MgO–$Al_2O_3$ phase diagram (Slag Atlas (1995)): (○) MA spinels with 0.5 wt% zirconium silicate, (△) MA spinels with 1.0 wt% zirconium silicate and (□) MA spinels with 2.0 wt% zirconium silicate; (●) MA spinels with 2.0 wt% chromite, (▲) MA spinels with 3.0 wt% chromite and (■) MA spinels with 5.0 wt% chromite.

Table 3
Representative microanalyses and mean density of spinel crystals from the synthesised spinel-based materials

| Oxides (wt%) | Samples | | | | | |
|---|---|---|---|---|---|---|
| | 0.5ZrS | 1ZrS | 2ZrS | 2Chr | 3Chr | 5Chr |
| $Al_2O_3$ | 70.85 | 71.02 | 69.31 | 67.78 | 66.80 | 65.97 |
| $TiO_2$ | 0.00 | tr | 0.00 | tr | tr | 0.00 |
| MgO | 27.30 | 27.84 | 27.64 | 27.51 | 27.92 | 27.20 |
| FeO | 1.38 | 0.51 | 0.68 | 0.46 | 0.004 | 0.80 |
| $Fe_2O_3$ | 0.00 | 0.23 | 2.48 | 1.18 | 2.23 | 1.83 |
| $Cr_2O_3$ | tr | tr | 0.00 | 2.55 | 2.95 | 4.19 |
| $ZrO_2$ | tr | 0.00 | 0.00 | 0.00 | 0.00 | 0.00 |
| Number of cations on the basis of 32(O) in formula | | | | | | |
| Al | 15.96 | 15.97 | 15.64 | 15.44 | 15.18 | 15.09 |
| Ti | – | – | – | – | – | – |
| Mg | 7.78 | 7.92 | 7.89 | 7.93 | 8.02 | 7.87 |
| $Fe^{2+}$ | 0.22 | 0.08 | 0.11 | 0.07 | 0.001 | – |
| $Fe^{3+}$ | – | 0.03 | 0.36 | 0.17 | 0.32 | 0.13 |
| Cr | – | – | – | 0.39 | 0.45 | 0.27 |
| Mean density of spinel crystals ($g/cm^3$) | 3.57 | 3.56 | 3.56 | 3.58 | 3.59 | 3.59 |

without chromium. The mean density values of spinel crystals from each sample have been calculated according to Cullity [13], with the results given in Table 3. Calculations of Gibbs energies using the program HSC OUTOCAMPU [14] reveals that $\Delta G_{MgOCr_2O_3} < \Delta G_{MgOAl_2O_3}$, suggesting that $Cr_2O_3$ acts as a core for the formation of the spinel, accelerating the sintering process. Furthermore as the amount of chromite additive increases, the spinel becomes more chromium rich, the direct diffusion bonding should be stronger, and a promotion of the resistance against the chemical corrosion from fused metallurgical slag would be expected.

The chemistry of periclase crystals was also determined by performing approximately 30 spot microanalyses in every sample, and representative data are listed in Table 4. Periclase crystals from the chromite added samples are lower in MgO than those from samples with a zirconium silicate additive, due to incorporation of small amounts of chromium (up to 0.84 wt% $Cr_2O_3$) and iron (up to 3.35 wt% FeO) in the MgO structure as a solid solution. The FeO content of the periclase crystals from the samples with zirconium silicate additive ranges between 0.83 and 2.02 wt%.

Table 4
Representative microanalyses of periclase crystals from the synthesised spinel-based materials

| Oxides (wt%) | Samples | | | | | |
|---|---|---|---|---|---|---|
| | 0.5ZrS | 1ZrS | 2ZrS | 2Chr | 3Chr | 5Chr |
| $Al_2O_3$ | 0.20 | 0.13 | 0.20 | 0.12 | 0.09 | 0.12 |
| MgO | 98.27 | 98.75 | 97.01 | 96.20 | 96.06 | 95.87 |
| FeO | 0.85 | 0.83 | 2.02 | 2.77 | 3.35 | 3.02 |
| $Cr_2O_3$ | tr | tr | tr | 0.23 | 0.25 | 0.77 |
| $ZrO_2$ | 0.00 | tr | 0.00 | 0.00 | 0.00 | 0.00 |

The rim chemical compositions of periclase-MA spinel pairs of crystals from the same sample, found in contact with each other, have been plotted on the MgO–$Al_2O_3$ phase diagram (Fig. 2) [15]. The data points reveal a good fit to both the MgO and $Al_2O_3$-poor spinel solvus of the diagram, suggesting that equilibrium was established in the grains. This figure also suggests that coexisting periclase-spinel pairs from the samples with chromite additive were possibly equilibrated

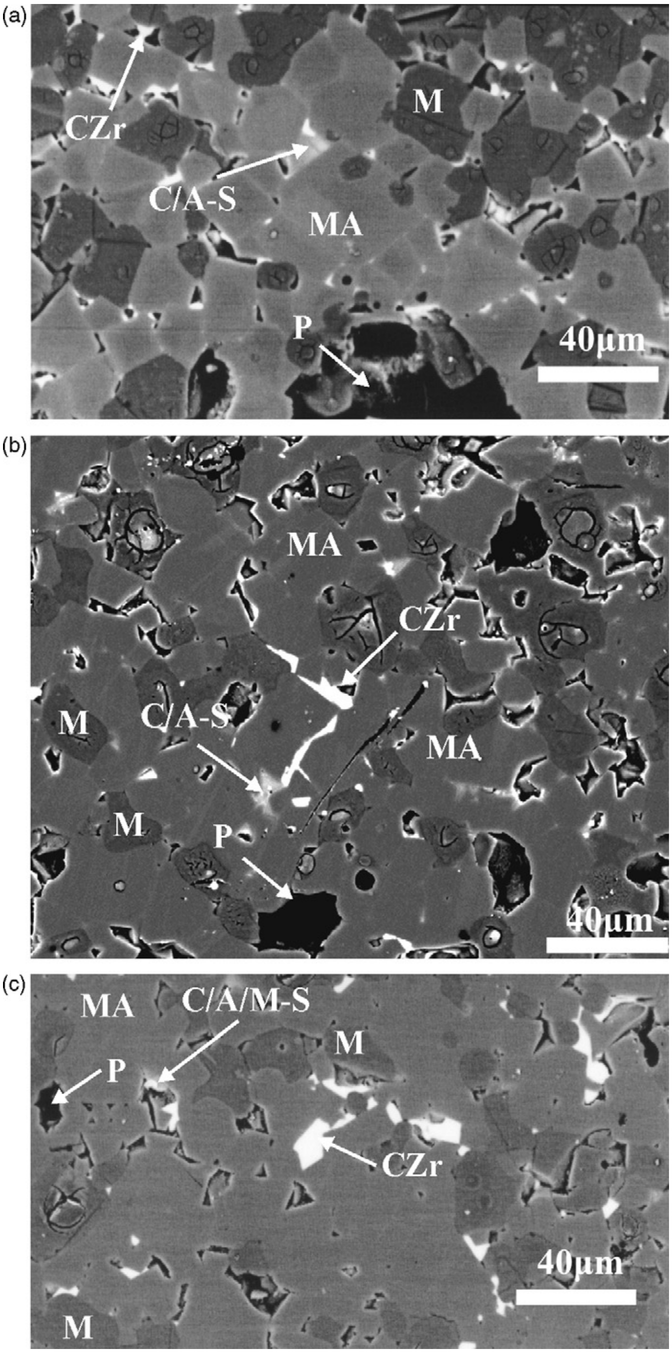

Fig. 3. Backscattered SEM photomicrographs showing the microstructure of M-MA spinel-based materials with zirconium silicate additives, after firing at 1760 °C. (a) 0.5 wt% zirconium silicate additive, (b) 1 wt% zirconium silicate additive, and (c) 2 wt% zirconium silicate additive. Dark gray (M) = periclase; light gray (MA) = spinel; white (C/A/M-S) = Ca or Al or Mg silicates; bright-white (CZr) = $CaZrO_3$; black (P) = pore.

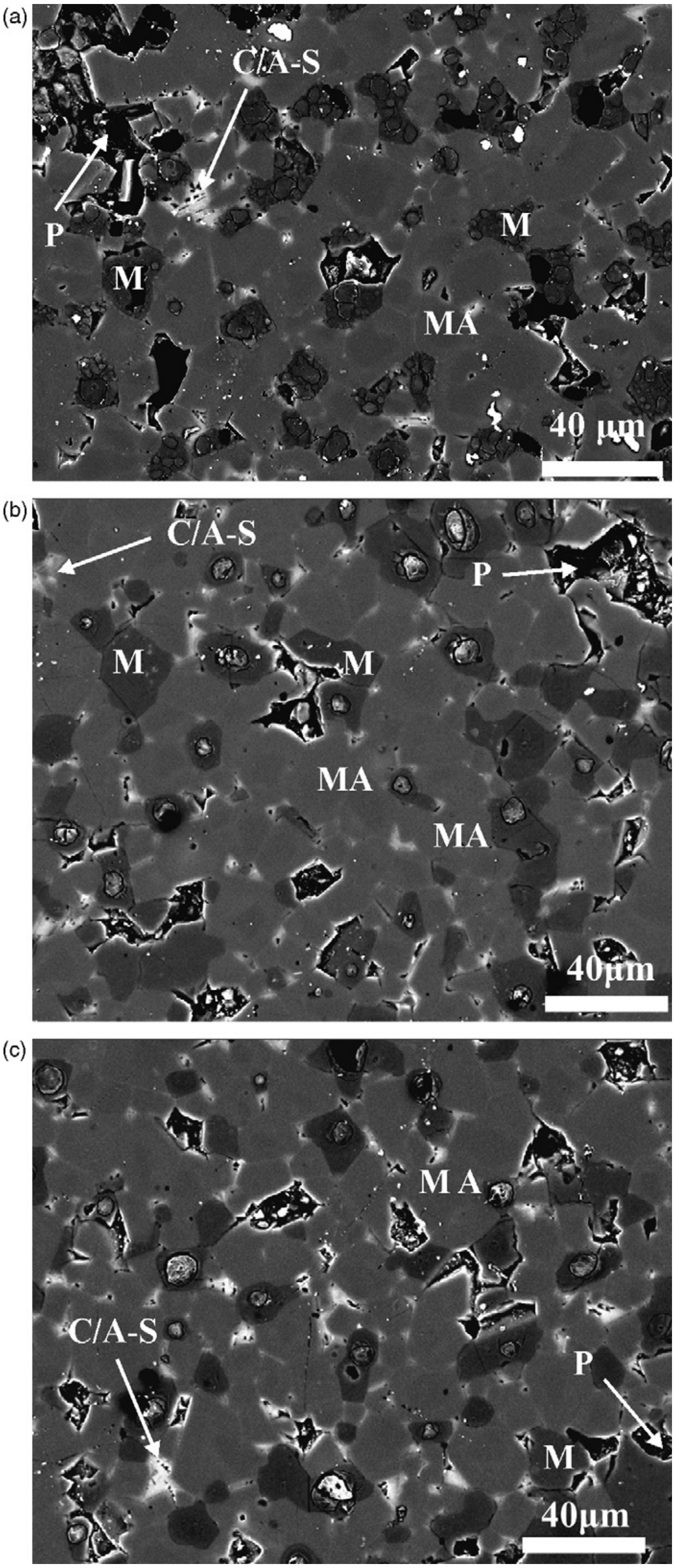

Fig. 4. Backscattered SEM photomicrographs showing the microstructures of M-MA spinel-based materials with chromite additives, after firing at 1760 °C. (a) 2 wt% chromite additive, (b) 3 wt% chromite additive, and (c) 5 wt% chromite additive. Dark gray (M) = periclase; light gray (MA) = spinel; white (C/A-S) = Ca or Al silicates; black (P) = pore.

at temperatures higher than those of the corresponding pairs from the samples with zirconium silicate as an additive.

A rough estimation of the equilibration temperatures for coexisting periclase-spinel pairs from the samples with zirconium silicate and chromite additive, obtained from Fig. 2, suggests temperatures ranging between 1600–1650 and 1650–1700 °C, respectively.

### 3.4. Microstructure

Backscattered images of spinel-based compositions with additives zirconium silicate and chromite are given in Figs. 3 and 4, respectively.

Both figures show that all the examined samples have a dense crystalline structure with a high rate of grain growth of spinel as well as direct bonding of the same crystals. The presence of free periclase noticed in all microstructures may hinder the grain growth of rounded spinel crystals.

The calcium–aluminate and calcium–silicate bonding phases which were traced in all six spinel-based compositions, occur in low amounts, mainly at the grain boundaries of spinel and periclase, so they practically do not reduce the refractoriness of the materials.

In samples with zirconium silicate, the proportion of the high melting point phase $CaZrO_3$ increases with the increase of the amount of additive, promoting densification, as well as the refractoriness of the materials (by filling pores).

On the other hand, in samples with chromite additives, the amount of low melting phases appears to be increasing slightly, but they still are encountered in low amounts, while the incorporation of chromium in the spinel lattice helps to increase the rate of strong, direct contact between the crystals.

## 4. Conclusions

Refractory samples of $MgO{\cdot}Al_2O_3$ spinels used in steelmaking and cement manufacture were prepared in a two stage sintering process with 0.5, 1.0, and 2.0 wt% zirconium silicate and 2.0, 3.0 and 5.0 wt% chromite ore additions. Changes in microstructure and chemistry of the crystalline phases indicated the following:

(1) In Mg–Al spinel-based materials with zirconium silicate additive, the refractory phase of $CaZrO_3$ was formed, promoting the hot strength resistance of the material at high temperature. As the amount of the zirconium silicate additive increased, the formation of the $CaZrO_3$ and calcium silicate phases increased, while the amount of calcium aluminate phases decreased. The addition of zirconium silicate to the spinel-based compositions indicated that the sample with 0.5 wt% additive had the lower bulk density (3.32 g/cm$^3$), while samples with 1.0 and 2.0 wt% have higher density (3.35 g/cm$^3$).

(2) XRD analyses, optical and SEM microscopy, and combined WDX-EDX quantitative elemental analyses of phases present in Mg–Al spinel with chromite as additive indicated that no Cr-bearing minor phase was present in the

microstructures. $Cr_2O_3$ mainly enters the MA spinel structure by solid solution, accelerating the spinel formation process, and improves the spinel crystals density as well as the strength of the direct spinel–spinel bonding. It was also found that the addition of comparatively small amounts of chromite is effective in increasing the bulk density of the compositions.

(3) Based on the microstructure, mineralogical composition, bulk density and spinel crystal density; MA spinels with 1.0 wt% zirconium silicate and with 5.0 wt% chromite additives are recommended as the most suitable for the production of high technology refractory materials. Use of zirconium silicates is considered to be more environmentally friendly because of the elimination of Cr.

## Acknowledgments

The authors wish to thank Mr. V. Kotsopoulos of the laboratory of Electron Microscopy and Microanalysis, University of Patras, for his help with the Microanalyses and SEM photomicrographs.

## References

[1] T.F. Baranova, I. Kurskaya, N.A. Dabizha, Sintering of high purity magnesia and magnesium aluminate, Ogneupory 46 (3) (1981) 54–56.

[2] L.A. Skomorovskaya, Magnesia spinel ceramics alloyed with rare earth oxides, Glass Ceram. 50 (3–4) (1993) 165–168.

[3] Y.H. Baik, Sintering of magnesium aluminate spinel and its characteristics, Yoop Hikhoechi 22 (6) (1985) 29–36.

[4] R. Sarkar, G. Bannerjee, Effect of addition of $TiO_2$ on reaction sintered $MgO–Al_2O_3$ spinels, J. Eur. Ceram. Soc. 20 (12) (2000) 2133–2141.

[5] R. Sarkar, S.K. Das, G. Bannerjee, Effect of additives on the densification of reaction sintered and presynthesised spinels, Ceram. Int. 29 (1) (2003) 55–59.

[6] A. Ghosh, S.K. Das, J.R. Biswas, H.S. Tripathi, G. Banergjee, The effect of ZnO addition on the densification and properties of magnesium aluminate spinel, Ceram. Int. 26 (6) (2000) 605–608.

[7] S. Ju, G.F. Fang, C. Xi-Ping, Effect of addition of $Cr_2O_3$ on slag resistance of magnesia\spinel refractory, Naihuo Cailiao 28 (4) (1994) 189–192.

[8] F. Li, L. Tan, Effects of additives on properties of unburned $MgO–Al_2O_3$ refractory, China's Refractories 8 (4) (1999) 12–14.

[9] X. Peng, K. Zhou, X. Zhang, Effects of $Cr_2O_3$ on properties of alumina-spinel castable, China's Refractories 8 (3) (1999) 6–8.

[10] R. Sarkar, S.K. Das, G. Banerjee, Effect of addition of $Cr_2O_3$ on the properties of reaction sintered $MgO–Al_2O_3$ spinels, J. Eur. Ceram. Soc. 22 (8) (2002) 1243–1250.

[11] M. Fujita, H. Yoshimatsu, A. Osaka, A. Miura, Preparation and properties of $ZrO_2$ disperse $MgO–Al_2O_3$, ceramics: effect of $ZrO_2$ content, Yoop Hikhoechi 103 (8) (1995) 838–843.

[12] D. Yang, H. Sun, J. Feng, S. Li, J. Ling, Effect of $ZrO_2$ additives on the thermal shock resistance of MgO-MA refractory, China's Refractories 9 (1) (2000) 25–28.

[13] B.D. Cullity, The determination of crystal structure, in: Elements of X-ray Diffraction, Addison-Wesley Publishing Company, Inc., 1959, pp. 297–323.

[14] A. Roine, P. Bjorklund, P. Riikonen: HSC of OUTOCAMPU chemistry for windows, chemical reaction and equilibrium software with extensive thermo chemical database, version 5.1, 2002.

[15] M. Allibert, Phase diagram of $MgO–Al_2O_3$, in: Slag Atlas (2nd ed.), edited by Verein Deutscher Eisenhuttenleute (VDEh), Press in Germany, 1995, 44 pp.